

4.4 CAVITATING JET CELLS

Erosion tests in Lichtarowicz cells were conducted in the Fluid Control Research Institute (FCRI), Palghat, India and at the University of Hannover (HAN lab), Germany. Specimens of Ø12 mm¹ and Ø14 mm diameter were used. However, due to lack of data on eroded area in Hannover, only the volume loss curves are reproduced in this section (Figs 29, 30). Nozzle diameters were close to the ASTM G134-95 standard values (Ø 0.408 ±0.004 mm). However, in both cases the tolerances applied (+ 0.015 mm) do not keep current requirements of the Standard². Basing on the FCRI results (Table 18a and Fig.30) one can suppose that even a scatter of 0.005 mm can have a meaningful effect on the results obtained³. Differences between results from two labs result also from different stand-off distances and different operating parameters applied.

Basing on the HAN data one can follow the erosion rate dependence on the cavitation number

$$\sigma = \frac{p_d - p_v}{p_u - p_v} \approx \frac{p_d}{p_u}$$

(Table 19, Fig.31). The ordering of materials usually follows the order of their appearance in Table 1. However, relatively poor performance of the carbon steel 45 at the Hannover University lab is an unexpected result. One should notice that the incubation period for this steel is fairly long which suggests fatigue as the main mechanism of erosion.

**Table 18a Test Series Summarisation Table of the FCRI cavitating jet cell
(upstream pressure⁴: 9.91 MPa, downstream pressure⁵: 0.24 MPa,
specimen dia: Ø12 mm , stand-off distance: 10 mm)**

Material	test duration	nozzle diameter	volume loss	eroded area	Incubation period	MDPR _{max}
	min	mm	mm ³	mm ²	min	µm/min
PA2	960	0.424	46.926	59.4	40	1.205
M63	1200	0.413	8.563	48.5	85	0.200
M63	1200	0.418	6.678	36.1	85	0.210
E04	1800	0.399 ⁵	9.825	40.0	200	0.178
45	2400	0.397 ⁶	5.338	33.7	187	0.092
1H18N9T	3000	0.424 ⁷	2.527	51.8	1350	0.027

¹ ASTM G134-95 standard

² It should be stressed that the tests under discussion were conducted several years before the Standard was established.

³ An unequivocal statement in this respect requires statistical processing of a number of tests under the same conditions.

⁴ absolute value

⁵ changed for Ø 0.414 after 20 hours of test

⁶ changed for Ø 0.413 after 20 hours of test

⁷ changed for Ø 0.416 after 20 hours of test

Table 18b Test Series Summarisation Table of the HAN cavitating jet cell
 (upstream pressure¹: 14.0 MPa, downstream pressure¹: 0.1 MPa,
 specimen dia: Ø14 mm, nozzle dia: Ø 0.4 mm, stand-off distance: 18 mm)

<i>material</i>	<i>test duration</i>	<i>volume loss</i>	<i>eroded area</i> ²	<i>incubation period</i>	<i>MDPR_{max}</i>
	min	mm ³	mm ²	min	µm/min
PA2	294	17.86	165.1	43.3	0.3175
M63	735	2.918	165.1	360.0	0.0650
E04	2671	8.226	165.1	283.0	0.0250
45	930	3.152	165.1	443.0	0.0350
1H18N9T	1805	2.270	165.1	416.6	0.0085

Table 18c Test Series Summarisation Table of the HAN cavitating jet cell
 (upstream pressure¹: 17.0 MPa, downstream pressure¹: 0.1 MPa,
 specimen dia: Ø14 mm, nozzle dia: Ø 0.4 mm, stand-off distance: 18 mm)

<i>material</i>	<i>test duration</i>	<i>volume loss</i>	<i>eroded area</i>	<i>incubation period</i>	<i>MDPR_{max}</i>
	min	mm ³	mm ²	min	µm/min
PA2	180	22.317	165.1	6.6	1.240
M63	368	3.250	165.1	230.0	0.155
E04	1620	10.730	165.1	160.0	0.053
45	687	4.588	165.1	300.0	0.083
1H18N9T	988	2.510	165.1	340.0	0.030

Table 18d Test Series Summarisation Table of the HAN cavitating jet cell
 (upstream pressure¹: 19.0 MPa, downstream pressure¹: 0.1 MPa,
 specimen dia: Ø14 mm, nozzle dia: Ø 0.4 mm, stand-off distance: 18 mm)

<i>material</i>	<i>Test duration</i>	<i>volume loss</i>	<i>eroded area</i>	<i>incubation period</i>	<i>MDPR_{max}</i>
	min	mm ³	mm ²	min	µm/min
PA2	120	23.245	165.1	6.0	1.380
M63	180	3.523	165.1	51.7	0.165
E04	617	6.711	165.1	100.0	0.088
45	643	9.138	165.1	265.0	0.143
1H18N9T	1322	5.884	165.1	156.7	0.031

¹ absolute value

² impinged surface area

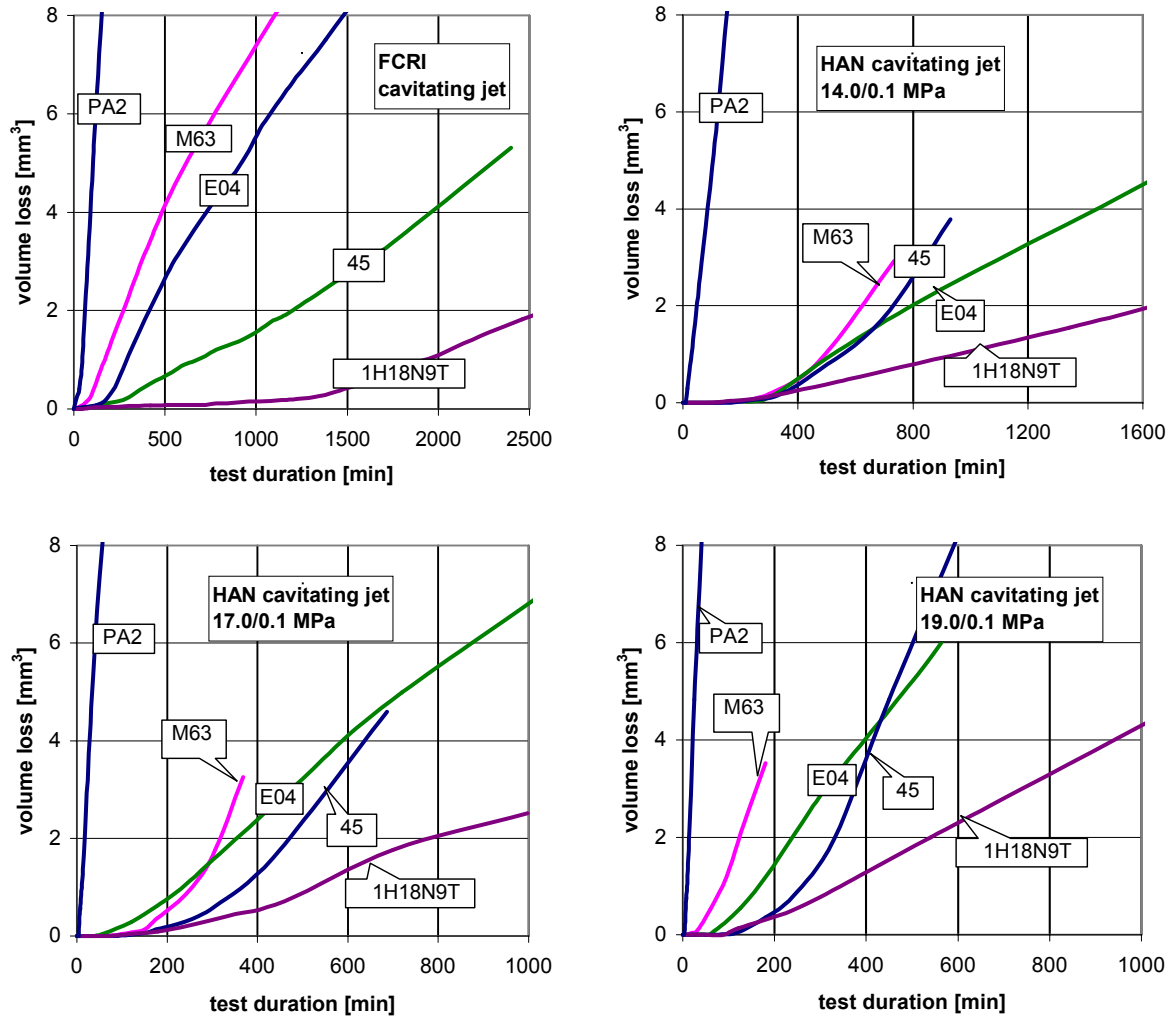


Fig.29 Cumulative volume loss curves of the ICET materials tested in cavitating jet cells

Table 19
Maximum values of the instantaneous erosion rate , mm³/h, in the HAN cavitating jet cell

<i>material</i>	$\sigma = 0.526 \text{ E-}03$	$0.588 \text{ E-}03$	$0.714 \text{ E-}03$
PA2	13.670	12.283	3.145
M63	1.634	1.535	0.644
E04	0.872	0.525	0.248
45	1.417	0.822	0.347
1H18N9T	0.307	0.297	0.084

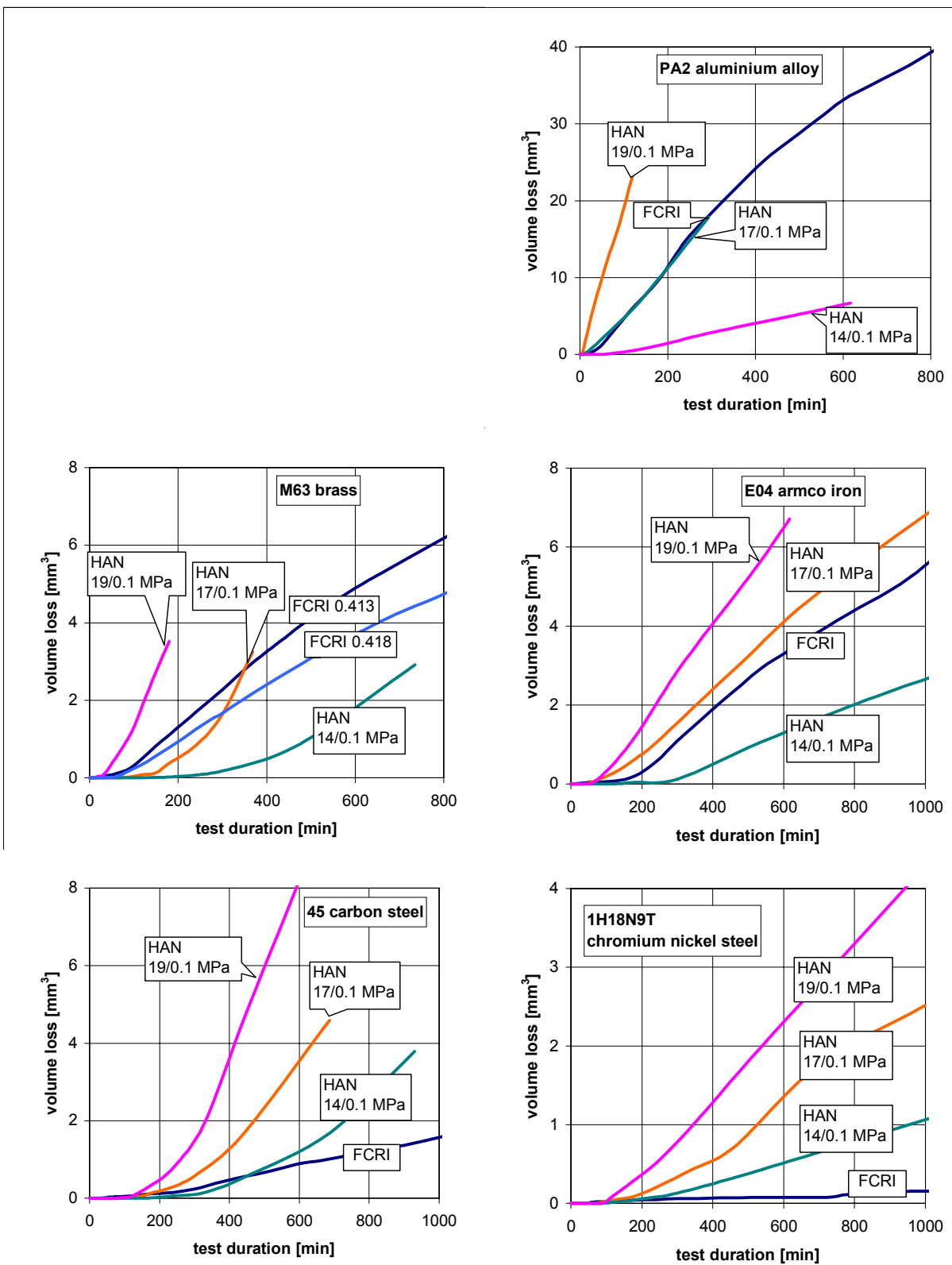


Fig.30 Cumulative volume loss curves of the ICET materials tested in cavitating jet cells

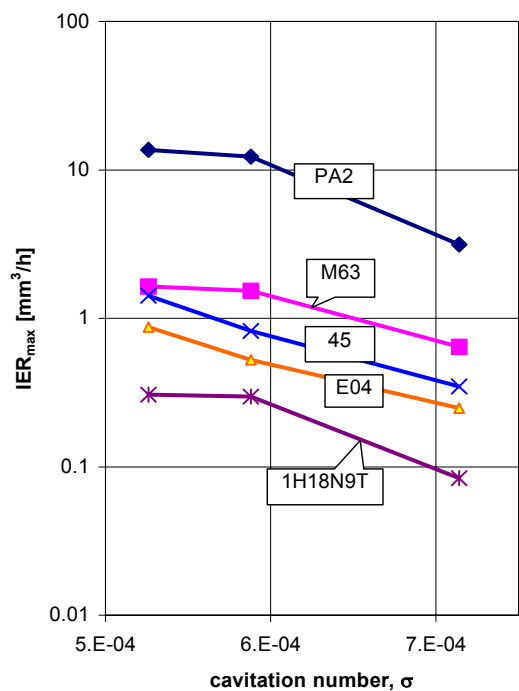


Fig.31 Maximum instantaneous erosion rates of ICET materials tested in the HAN cavitating jet cell at various cavitation numbers

By comparing the FCRI and HAN results (Fig.30), one can easily notice an excellent coincidence of the volume loss curves of PA2 alloy tested in Palghat with one of curves determined in Hannover (17 MPa upstream pressure). However, with rising resistance, the erosion rate of materials tested in FCRI falls gradually in respect to that in Hannover. Erosion rate of the 1H18N9T stainless steel tested in FCRI is substantially smaller than that in Hannover for 14.0 MPa upstream pressure. One may suppose that a high number relatively weak cavitation pulses in Palghat is responsible for intense erosion of PA2 and M63. The amplitude of this pulses may be however insufficient to generate intense erosion in highly resistant materials.